6-2021

Radio Frequency Direction Finding System

Jacob Taub

Austin Colon

SANTA CLARA UNIVERSITY

Department of Electrical and Computer Engineering

I HEREBY RECOMMEND THAT THE THESIS PREPARED UNDER MY

SUPERVISION BY

Jacob Taub, Austin Colon

ENTITLED

RADIO FREQUENCY DIRECTION FINDING SYSTEM

BE ACCEPTED IN PARTIAL FULFILLMENT OF THE REQUIREMENTS
FOR THE DEGREE OF

BACHELOR OF SCIENCE
IN
ELECTRICAL ENGINEERING

June 4 2021

Thesis Advisor date

Shoba Krishnan June 4th 2021

Department Chair date

Acknowledgements:

Special thanks to Dr. Kurt Schab who has invested an incredible amount of time into teaching us most of what we know about electromagnetics and always provides great feedback and suggestions regarding this project. Also, thanks to all of the other faculty at Santa Clara University who have helped us along our educational journey.

Abstract:

In certain terrain types It is difficult to locate people, objects, animals, etc. In particular, using one's eyes and ears to locate something has certain disadvantages. Visible light propagates at high frequencies and is easily stopped by terrain. Also, sound waves do not propagate as effectively as electromagnetic waves in open air because they are mechanical waves. Therefore, our goal is to create a system that can locate emitters that output electromagnetic waves in the radio frequency (RF) portion of the electromagnetic spectrum (EMS). RF operates at a lower frequency than visible light and will diffract around mountains and pass through jungle foliage more easily than light. The goal of this project is to design a system that will be compact, lightweight, and provide a signal strength/clock direction output pair to the operator indicating where the target emitter is located. Thus far we have been able to design and build a prototype system that accomplishes most of our goals. Tests with our prototype system have shown that our design concept is realizable given our system is lightweight and provides the operator with a bearing and signal strength of a target emitter. However, due to issues with our motor and motor controller, our system is unable to achieve our desired accuracy. Overall, the predominant issues we have encountered are our motor controller and motor being too weak to rotate our antenna. This issue may be remedied by increasing our budget slightly and incorporating a more powerful motor and better quality motor controller. Given the incorporation of an improved motor controller and motor, our system should be able to meet all of our original design objectives and be finalized into a compact usable product.

Table of Contents:

List of Figures & Tables:

1 Introduction:

1.1 Problem:

Generally, depending on a variety of factors, it can be challenging to locate things. There are nearly infinite applications that can involve locating things and generally application choices are only limited by the operator's creativity. However, for explanatory purposes, the applications discussed in this section will be broken down into two categories: government and commercial.

Common government applications include military and law enforcement applications. Military applications typically include: tracking enemy combatants, locating and rescuing downed pilots, and using RF direction finding (DF) systems to enhance communication links. Enemy combatants typically use some form of radio communications. Thus, friendly military forces with RF DF systems can locate and monitor enemy combatants by locating their communication equipment. Pilots may also be equipped with a beacon in the case that they are shot down. This beacon will transmit on a known channel that a search and rescue team equipped with an RF DF system can use to locate said pilot. Communications links can be enhanced using RF DF systems by locating which direction a signal is being received from and then pointing a directional receive antenna in that direction. Also, some examples of law enforcement applications include enforcing Federal Communications Commission (FCC) operating restrictions for emitters and locating criminals.

Common commercial applications include search and rescue, tracking wildlife, and enhancing communication links. Most of these applications involve using some sort of beacon operating at a known frequency. A specific example of a commercial application is bird watching. This process involves attaching small RF tags to certain birds and then releasing them within a wildlife preserve. The bird watcher can then periodically return to the preserve and use an RF DF system to locate their target bird. An example of one of these systems is shown below in Figure 1:

Figure 1: Bird tracking handheld RF DF system [1]

1.2 Statement of Project:

The goal of this project was to design a compact, portable, multi-platform RF DF system. This system was designed to provide options for both real-time readouts and aggregated measurements for post-processing analytics by geotagging a line of bearing (LOB) and received signal strength (RSS) of target signals.

1.3 What is Radio Frequency Direction Finding?:

RF DF is the act of locating emitters that output signals in the RF part of the electromagnetic spectrum (EMS). The RF spectrum is typically considered to be the frequency range of 20 kHz to 300 GHz. This frequency range is where alternating current (AC) can cause energy to radiate off of a conductor in the form of radio waves. A breakdown of the RF part of the EMS spectrum is shown in Figure 2 below:

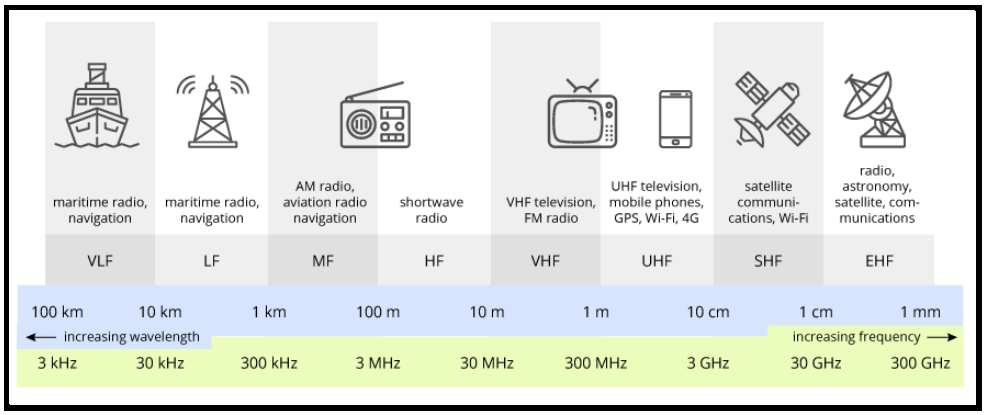

Figure 2: Common applications within the RF portion of the EMS [2]

Figure 2 outlines common applications that occur within the RF spectrum. Most people encounter applications that use the high frequency (HF), very high frequency (VHF), ultra-high frequency (UHF), and super high frequency (SHF) ranges of the RF spectrum within everyday life. Amplitude Modulated (AM) and Frequency Modulated (FM) radio, what someone typically listens to in a car, operate in the MF (550-1720 kHz) and VHF ranges (88-108 MHz) respectively. Cell phones typically operate in the UHF range in the United States (700 MHz, 850 MHz, and 1900 MHz) and Wi-Fi routers operate in both the VHF and UHF ranges (2.4 GHz, 5 GHz). An RF DF device would be used to locate any of the devices outputting signals in the RF range. Generally, as time has progressed, RF DF methods have increased in accuracy [3] but this has come at a cost. With increased accuracy there has also been an increase in complexity, processing, and power requirements.

1.4 Commercially Available Systems:

There are a variety of handheld RF DF systems available on the market. Many of these systems are cumbersome and require frequent physical adjustment by the user. One example is the Wolfhound RF DF [4] system employed by the United States Marine Corps (USMC) and United States Army for tactical RF DF operations. This system is shown in Figure 3 below:

Figure 3: Wolfhound RF DF system used by United States Military for tactical RF DF operations [5]

The Wolfhound consists of the following components: host controller box, handheld UI via personal digital assistant (PDA), antenna head, and adjustable mast. This system plus two BB-2590 batteries weighs around 15 pounds. This system is designed to be used in conjunction with a mast equipped backpack. The controller box is stored inside the backpack with cables running to the PDA and antenna head located on the mast. The antenna head also has 8 elements attached to it. Overall, the combination of weight, cabling, and protruding elements makes the system awkward and unwieldy. Also, when necessary, the operator must have another person raise or lower the mast for them or remove the backpack to make adjustments themselves. This is inconvenient. Many civilian RF DF systems have similar problems to the Wolfhound. Some civilian DF devices require the user to manually turn themselves or rotate an antenna in order to generate a LOB. Our proposed design addressed the issues presented by being compact, lightweight, and self contained.

1.5 Objectives:

Our system had the overarching goals of being compact/lightweight and easy to use. We planned to achieve the compact/lightweight goal by keeping our system weight under three pounds and containing it within a box of physical dimensions less than 5’’X5’’X4’’. To meet

these constraints we kept our processing requirements and power consumption low with the intent of being able to run our system off of six AA batteries for at least six hours. In order to make our system easy to use we decided to display DF data as an RSS value and associated LOB. The RSS is presented in a dBm value and the LOB as a degree bearing relative to magnetic north. A more advanced display was also planned to geotag individual measurements and be able to display them on a mapping software. As far as targeting is concerned, the goal of our system was to locate a one watt transmitter within the 5 GHz Unlicensed National Information Infrastructure (U-NII) band up to 200 meters away with an angle-of-arrival measurement of less than six degrees. These key objectives are outlined in Figure 4 below:

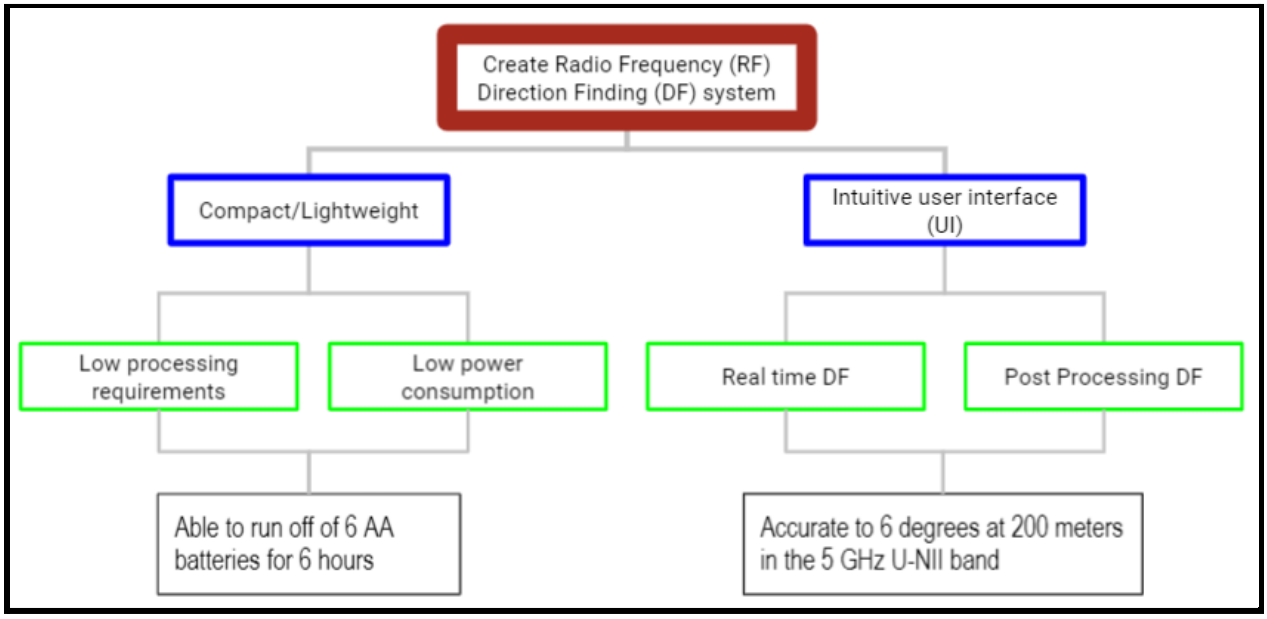

Figure 4: Key system objectives

2 Project Plan:

2.1 Anticipated Outcome:

Our goal was to design and build a system capable of meeting our objectives. The system was designed to be used for real time and a posteriori analysis direction finding applications. Real time direction finding instantaneously displays data directly to the user. Post processing

direction finding allows the user to run the system, record data over a period of time, and then dump the recorded data to a mapping software for interpretation. The goal of our post processing direction finding application was to produce an image like that shown below in Figure 5.

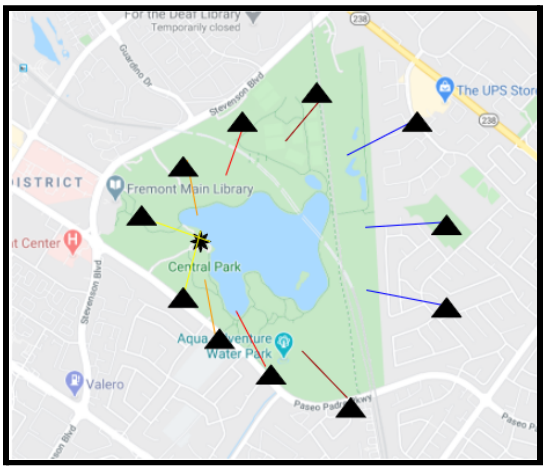

Figure 5: Concept image featuring GPS measurements with LOB indicators

Mapping software would display the geographic position of the measurement, received signal strength, and line of bearing attached to it. This would allow users to triangulate locations of target emitters by comparing measurements from multiple locations. This is important for situations in which the transmitter cannot be physically reached. An example of this would be trying to locate the beacon of a lost hiker that is buried in the snow or high up in steep mountainous terrain.

2.2 Implementation Choices and Tradeoffs:

There are numerous methodologies employed to locate RF emitters in the world today. When determining how best to meet our project goals we decided to study a few of these methods in order to make an informed decision on which one to implement. The two dominant methods employed are algorithm-based and receive signal strength (RSS)-based. Algorithmic methods involve using predetermined parameters of a known antenna array to solve for the angle of arrival of the system. The most commonly used algorithm is Estimation of Signal Parameters via Rotational Invariance Techniques (ESPRIT) [6], with Multiple Signal Classification

(MUSIC) [7] being a close second. A much more simplistic technique than the algorithmic methods mentioned above is the RSS method. The RSS method is an older concept that relies on physically moving a directional antenna to find the direction which produces the strongest signal.

When choosing between an algorithmic method or the RSS method the primary tradeoff we considered was power consumption. Both algorithms require significantly more power than the RSS implementation. The advantages to using these algorithms is that they can be constantly measuring, making them better at tracking moving sources. These algorithms will also provide higher accuracy measurements than the RSS method. However, for this design we are not trying to track moving targets, and instead are going for discrete measurements of the target's location. Thus, we ended up choosing the RSS method of RF DF. This helped us with meeting our battery life goal since the algorithmic methods are power intensive to run. Given that our system only needs to be able to generate LOB's within an accuracy of six degrees, the added accuracy from the algorithmic methods is not required. Another downside to the algorithmic methods is that they require known qualities of the antenna array. This would require calibration more often, meaning more actions to take for upkeep and maintenance.

A motor was used to physically move our antenna between RSS measurements. For the motor, we had to choose between two different options: a stepper motor and a servo motor. The basic trade off is that a servo motor would give a wider range of control for the system, while also requiring a control system to operate, while a stepper motor did not require a control system, but was limited in the number of angles it could take. Given that our goal in designing this system was simplicity and also the fact that we did not require an extremely wide range of control we decided to implement a stepper motor. The discrete steps of the motor also provided us with an advantage in that we could use it as a means of determining how many degrees were rotated between measurements.

2.3 Conceptual System Design:

After we defined our overarching system goals, chose the RSS RF DF method, and conducted some research, we determined how to specifically implement said method. We decided to use a directional antenna with an extremely narrow horizontal beamwidth and

implement the RSS method by rotating said antenna 360 degrees. As the antenna was rotated, received signal strength measurements were recorded and reported to a microprocessor. The microprocessor then selected the direction with the greatest signal strength within one 360 degree rotation as the direction of the target emitter. This process is illustrated below in Figure 6.

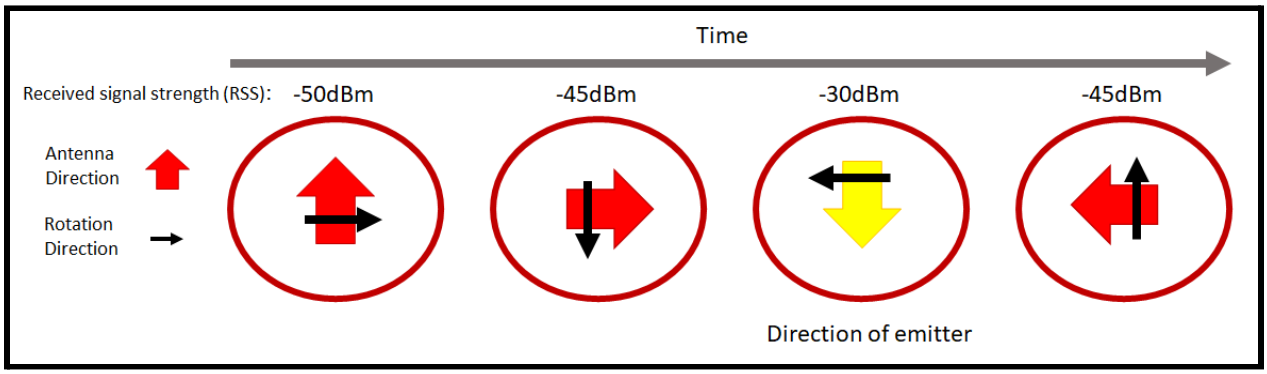

Figure 6: RSS method via rotating a directional antenna 360 degrees in the clockwise direction. Yellow arrow indicates direction of target emitter.

2.4 Block Diagram:

Our conceptual system design was decomposed into different functional blocks. A block diagram of our design is shown below in Figure 7.

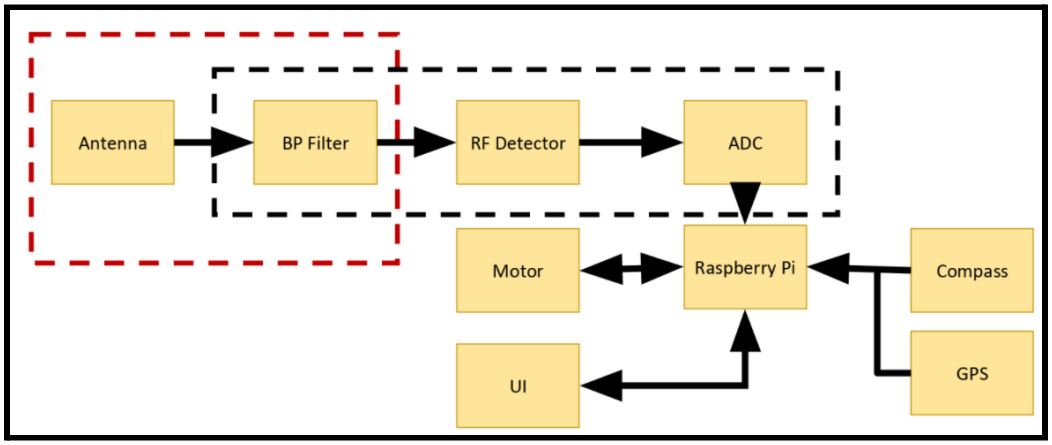

Figure 7: Block diagram of design. The components outlined with a dashed box are logical components that may be combined physically within our design.

First, the system received a signal via a highly directional patch antenna array that also acted as a bandpass (BP) filter. This antenna was attached to a stepper motor that rotated it and was controlled via our Raspberry Pi microprocessor. The received signal was then passed from the antenna to a universal serial bus (USB) network interface card (NIC) where it was filtered, converted to a voltage, and then from an analog to digital signal. The USB NIC effectively acted as a BP filter, RF detector, and analog to digital converter (ADC). The digital signal was then passed from the USB NIC to the Raspberry Pi to be interpreted. The Raspberry Pi then took the RSS as well as inputs from the compass and global positioning system (GPS) and then passed it to the user interface (UI) .

2.5 Division of Labor:

Our group decided to adapt a divide and conquer strategy when dividing up the workload associated with this project. We used our block diagram to identify each individual logical component and then broke them up into three different categories: joint tasks, Austin-specific tasks, and Jacob-specific tasks. This concept is illustrated in Figure 8 shown below:

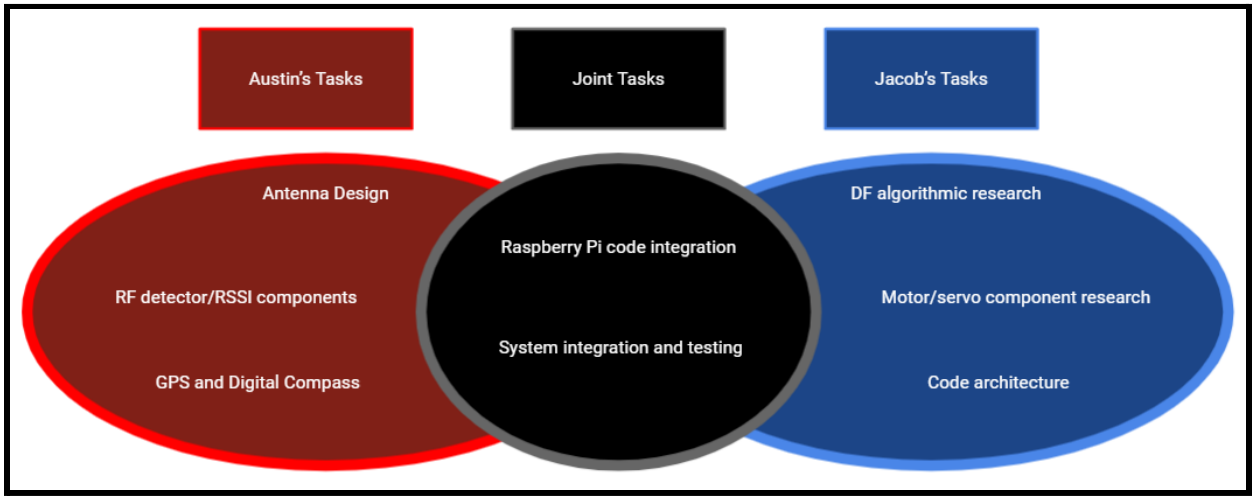

Figure 8: Division of tasks for RF DF system

Generally, the more difficult and complex tasks were allocated as joint tasks. The more specific tasks on researching individual components were divided up amongst each group member. This strategy allowed us to most effectively utilize our time and meet our design goals within our

project deadlines.

2.6 Methods:

Our goal was to first outline what we wanted our system to accomplish. After that, we conducted preliminary research and conceptualized a design to meet our objectives. Subsequently, we broke up our design into logical components and outlined a block diagram. With each component outlined we then divided up work on individual pieces of our project. As pieces were designed and assembled they were also individually tested. When certain combinations of pieces were completed they were tested jointly. The overarching goal of this approach was to start with a big picture idea, break it into smaller pieces, build the small pieces, and then assemble the system as a whole. This approach allowed us to identify problems easily and adjust our design as necessary. Also, it helped facilitate conducting work on this projectly jointly despite not being co-located.

In order to design the RF components of our system (Antenna/BP filter) we first started with a textbook design process [8, 9]. Next, we implemented some aspects of our design via Matlab and ran full wave electromagnetic simulations in Ansys HFSS to verify the performance of said design.

A Raspberry Pi was selected as the primary processing unit for this project. Data and controls for all components were grouped together using Python programming. This presented some integration challenges. First we had to familiarize ourselves with the capabilities and layout of the Raspberry Pi. This was essential in order to pick and integrate the other components of our system. In particular, we had to identify how our different peripheral components would interface with the Raspberry Pi while also meeting our size, power, and weight objectives. This involved research into the size, weight, and power consumption requirements for our motor, GPS, digital compass, and USB NIC. After this research was completed, peripheral components were selected and distributed to the appropriate group members. Subsequently, individual tests were conducted on each component and sub functions were created via Python. Lastly, everything was combined into a single system with a main code and associated sub functions. The system was then tested to see if design objectives were met.

2.7 Implementation and Test:

In this section each individual system component will be described in detail. Design rationale, processes, testing, and relevant sub functions will be discussed under each component sub header.

2.7.1 USB NIC:

We chose to initially use the EP-AC1635 [11] as our USB NIC. The EP-AC1635 is a plug and play USB WiFi adapter that is designed for personal electronic devices such as laptop computers. When choosing a USB NIC we had to take the following specifications into consideration: operating frequencies, receive sensitivity, and if it had an external antenna port or not. The EP-AC1635 was capable of receiving our target emitter frequency of 5.18 GHz, met the required receive sensitivity to ensure receiving a one watt signal at 200 meters was possible (this was calculated by using the provided receive sensitivity value and the Friss transmission formula), and also had an external RP-SMA port to attach our antenna to. However, even though it was advertised with driver support for Linux, the EP-AC1635 did not work with the Raspberry Pi. Thus, after emailing the manufacturer and getting no reply, we had to switch to a different USB NIC. However, we did learn from our mistake and specifically picked a more well known company that created USB NICs and ensured they had driver support for Linux. The USB NIC we chose was the AWUS036ACS [12]. This NIC also met all the requirements that the EP-AC1635 did. The two discussed USB NICs are shown below in Figure 9:

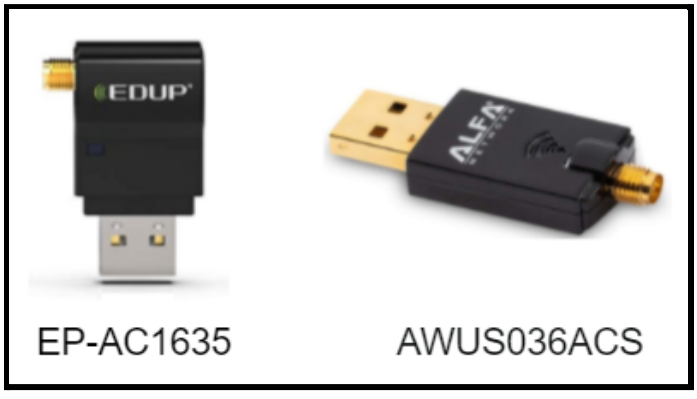

Figure 9: Old USB NIC (left) and new USB NIC (right)

The choice to use a USB NIC instead of piecemealing together a BP filter, RF detector, and ADC had some key benefits. First, it ensured all three of these components were enclosed in a compact and lightweight form. Second, it provided some extra capabilities such as the ability to target another channel in the 5 GHz U-NII band if necessary. Lastly, this is something that is easily recognizable and interfaceable by the Raspberry Pi. It provides a simple "plug and play" operation. Subsequently, all that was required to get this component to interface with our system was to be able to pull RSS values from it via Python.

2.7.1.1 USB NIC Test:

Testing the USB NIC involved inserting it into a functional computer/laptop and evaluating its connection to a local WiFi router. We were able to conduct a test using the vendor provided 3 dBi monopole antenna and comparing the expected signal strength value vs the measured signal value at one meter. Our emitter radiated an approximately 23 dBm signal with an assumed 3 dBi monopole. Thus, taking this into consideration, as well as assuming we are operating in a free space path loss environment we end up with the following values depicted in Figure 10 below:

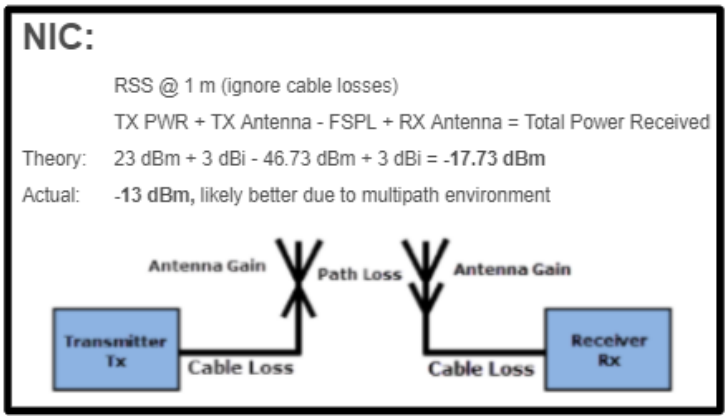

Figure 10: RSS test at one meter

From Figure 10 we can see that theoretically we should be receiving the signal at -17.73 dBm and our actual signal strength was -13 dBm. This is better than the theoretical value and indicates

that our USB NIC is functioning appropriately.

2.7.1.2 USB NIC Sub Function:

Overall, most of our sub functions were provided by the manufacturers of the components we purchased and were only modified slightly. However, one of the functions that did require a lot of work was the RSS sub function. The RSS sub function worked directly with the USB NIC. This function generally had two basic steps. First, it used the iwlist scan linux utility to display all WiFi access points received by the USB NIC. Next, this list was parsed based on the access point name and the RSS value was returned. A screenshot of the iwlist scan output is shown below in Figure 11 with the key fields outlined:

Figure 11: iwlist scan output showing target access point

The approach of targeting based on access point name was chosen because it allowed our system to potentially resolve the issue of co-channel interference. As long as the emitter signal is strong enough to decode the access point name, our system should be able to target it. This was tested in a signal dense environment with over 150 different access points and allowed us to locate the appropriate target.

2.7.2 Motor/Servo:

Our stepper motor was designed to be used in conjunction with the Raspberry Pi and a special stepper motor HAT that fits on top of the Raspberry Pi.

2.7.2.1 Stepper Motor:

For our stepper motor we decided to choose the Nema 17 stepper motor [13]. This motor provided us with a step angle of 1.8 degrees. While this did not exactly match up with our desired turn angle of 6 degrees, it did work nicely because it gave us a slightly more accurate measurement angle near 6 degrees if we so desired. This motor also did not require a lot of power to operate, especially given that we did not approach its upper limits of RPM. Also, this motor is not particularly heavy (390 g) which aligned with our goal of keeping our system as light as possible. The Nema 17 stepper motor is shown below in Figure 12:

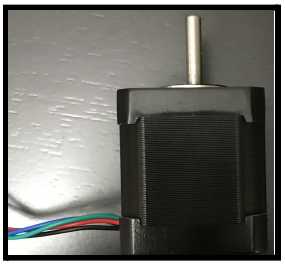

Figure 12: Nema 17 stepper motor side view

2.7.2.2 Stepper Motor Hat:

For our stepper motor HAT we decided to use the Adafruit DC and stepper motor HAT for Raspberry Pi mini kit [14]. The stepper motor HAT is designed to interface a Raspberry Pi with a stepper motor. It has a dedicated PWM chip that can potentially allow the Raspberry Pi to control up to two stepper motors with only two pins. Also, the stepper motor HAT provided isolation for the stepper motor and allowed it to be powered by its own supply independent of the Raspberry Pi. The stepper motor hat is shown below in Figure 13:

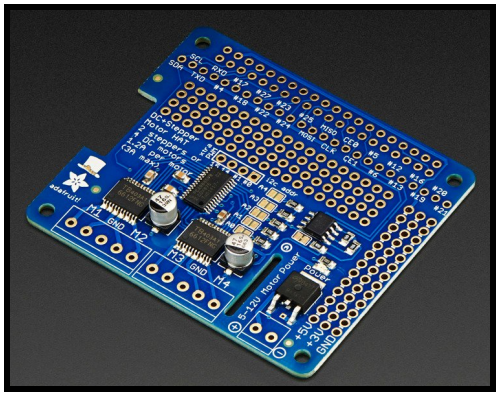

Figure 13: Adafruit DC and stepper motor HAT top view

2.7.2.3 Motor/servo test:

The stepper motor and stepper motor HAT were tested in conjunction by connecting them to the Raspberry Pi and commanding the Stepper Motor to rotate 360 degrees. This test was successful and proved that both components have baseline functionality. A second test we conducted that tested the stepper motor's ability to rotate with the antenna mounted to the end of it. This checked the ability of the stepper motor to rotate against the added weight and bulk of the antenna. Unfortunately, we were only able to get sporadic performance with the antenna mounted to the motor. This indicates that our motor is too weak. Stills of the antenna being rotated on the motor are shown below in Figure 14:

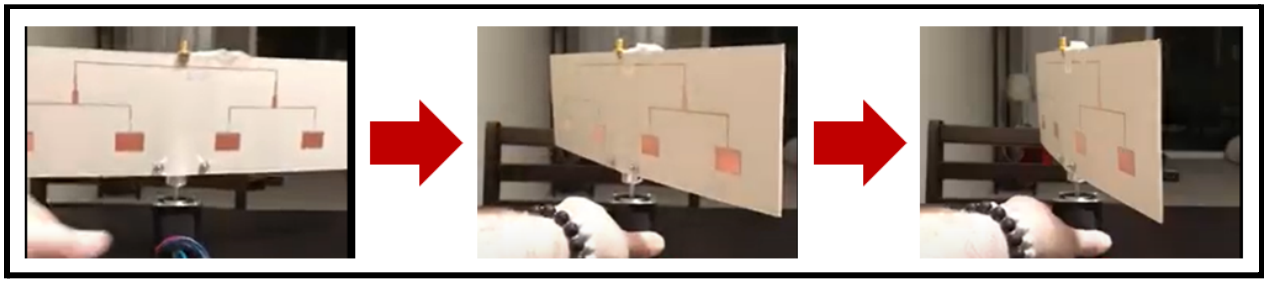

Figure 14: Stepper motor struggling to rotate antenna 360 degrees in the clockwise direction

2.7.2.4 Motor/Servo Sub Functions:

The function to run the motor through our HAT was implemented using the Circuit

Python package for Python that was provided by our HAT manufacturer. The package included a one line command to cause the stepper motor to step: stepper1.onestep(). The motor rotate function consists of three calls of this command to rotate our motor the desired number of degrees, then exit the sub function.

2.7.3 Microprocessor:

For our microprocessor we chose the Raspberry Pi 3 model B+ [15]. A Raspberry Pi is a common choice to use as the computer for many applications. The Raspberry Pi 3 Model B+ was selected for the microprocessor role because it is modern and has been extensively utilized/tested. The decision was made to not use the most recent model Pi (Raspberry Pi 4) because the power requirements for it were higher and the new features provided by it were not necessary for the project. This Raspberry Pi 3 Model B+ has four USB ports to interact with. This was adequate to interface all of the required USB peripheral devices. In order to avoid issues, it was decided to use Raspbian as the operating system for our Raspberry Pi as it is specifically designed to be used with Raspberry Pi's. The Raspberry Pi model 3 B+ is shown below in Figure 15:

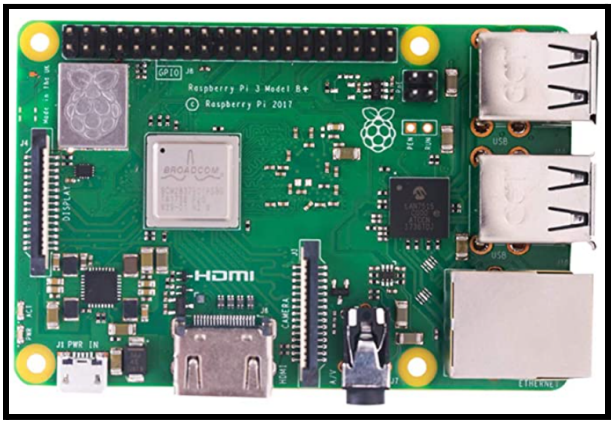

Figure 15: Raspberry Pi model 3 B+ top view

2.7.3.1 Microprocessor Test:

The test of our microprocessor was incredibly simple. We powered on the Raspberry Pi and ensured the operating system was loaded properly. Next, all four of the USB ports were

checked to see if they worked properly by connecting different devices to the Raspberry Pi (GPS, USB NIC, USB Mouse, etc.) and ensuring that said devices could communicate with the Raspberry Pi and operated properly. These tests were conducted successfully which indicated that our Raspberry Pi works properly.

2.7.4 Electronic Compass:

For the electronic compass, the Grove 3 Axis Digital Compass V2 [16] was selected. The electronic compass is essential to reliably determine the direction of our measurements. Instead of relying upon theoretical measurements of how much the motor actually turned, a measurement of the bearing of the front of the antenna was taken via the electronic compass. This piece was mounted with the antenna on the motor and spins with it to generate the correct directions. The Grove 3 Axis Digital Compass V2 was specifically chosen because it was inexpensive, small, lightweight, and easy to use/interface. The electronic compass is the only component that interfaces to our Raspberry Pi via general purpose input-output (GPIO) pins using the inter-integrated circuit (I2C) serial communications protocol. The Grove 3 Axis Digital Compass V2 is shown below in Figure 16:

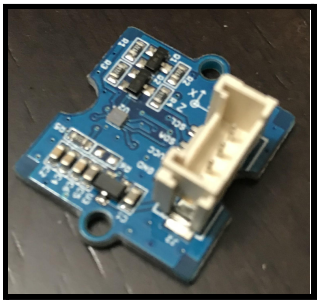

Figure 16: Grove 3 Axis Digital Compass V2 top view

2.7.4.1 Electronic Compass Test:

We first checked the electronic compasses functionality by plugging it into our Raspberry Pi and used the generic vendor supplied code to ensure that readings were continually output to a terminal. Next, we modified said code such that it output the y-axis (front of the compass) direction every 3 seconds, rotated the electronic compass, and checked to see if the readings

adjusted accordingly. This test was performed by hand and is depicted in Figure 17 below:

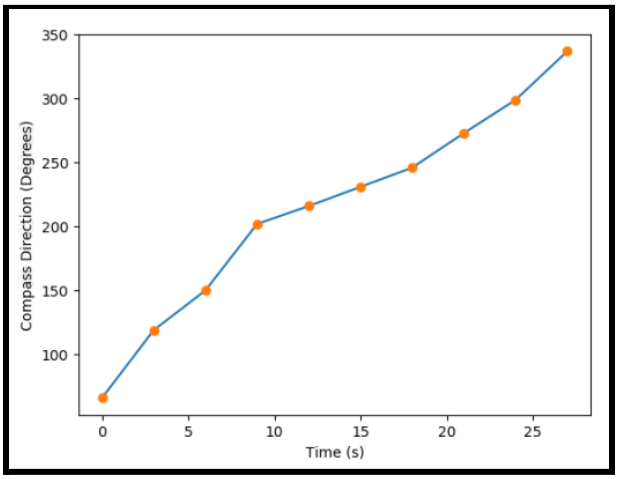

Figure 17: Hand rotated compass test. Compass rotated at roughly constant speed in 360° rotation, with the graph showing the time spent rotating vs the direction faced.

From Figure 17 we can see one full 360 degree hand rotation. From this we can deduce that our compass functions appropriately because there is a nearly linear relationship with the compass values increasing from 0 to 360 degrees over a single rotation.

2.7.4.2 Electronic Compass Sub Function:

The vendor provided electronic compass function provides users with an x, y, and z direction bearing as well as some magnetic properties. For our purposes, we only need the y direction which indicates the front of the compass. Thus, our function asks the electronic compass for the direction it is facing (y direction), and returns the angle the compass is facing, where 360°/0 ° is North.

2.7.5 GPS:

For our GPS we chose the GlobalSat BU-353-S4 USB GPS Receiver [17]. The GPS unit is essential for our post processing goals. For us to produce a map with the points where RSS measurements were taken, we need to know the latitude and longitude associated with said measurements. The GPS allows us to do that. We chose this unit because it is compact,

lightweight, accurate, and can interface with one of the USB slots on the Raspberry Pi we are using. The GlobalSat BU-353-S4 is shown below in Figure 18:

Figure 18: GlobalSat BU-353-S4 top view

2.7.5.1 GPS Test:

We tested the GPS by plugging it into our Raspberry Pi and checking the latitude and longitude readings we obtained. To verify the accuracy of said readings we plotted the GPS coordinates on Google Maps and checked to see if they were close to the known location that the reading was taken from. From our GPS we were able to receive a latitude and longitude within four decimal places of what was expected based on Google Maps. This indicated that our GPS was within 11 meters of the expected value and seemed to be functioning appropriately.

2.7.5.2 GPS Sub Function:

Our GPS sub function was created around reading the serial data stream collected and reported by the GPS to the Raspberry Pi over USB. After connecting the GPS, it will power on and then continually stream data until it is unplugged or the Raspberry Pi loses power. This data stream can be accessed through a GPS service daemon called gpsd. The GPS sub function is set up such that each time it is called it pulls the most recently reported latitude and longitude values from gpsd and returns them as floats in Python.

2.7.6 Antenna:

In order for the RSS method that was outlined in our conceptual design section to be

effective, a narrow horizontal beamwidth was required. A narrow horizontal beamwidth was necessary because it caused the RSS value to significantly increase when the antenna was pointed directly at the emitter and to noticeably decrease when the motor rotated the antenna away from the emitter slightly. Thus, our design goal was to create an antenna that was both compact and had a highly directional horizontal radiation pattern. Based on these design criteria we decided to use a linear array of edge fed half-wavelength microstrip patch antennas. This is shown below in Figure 19.

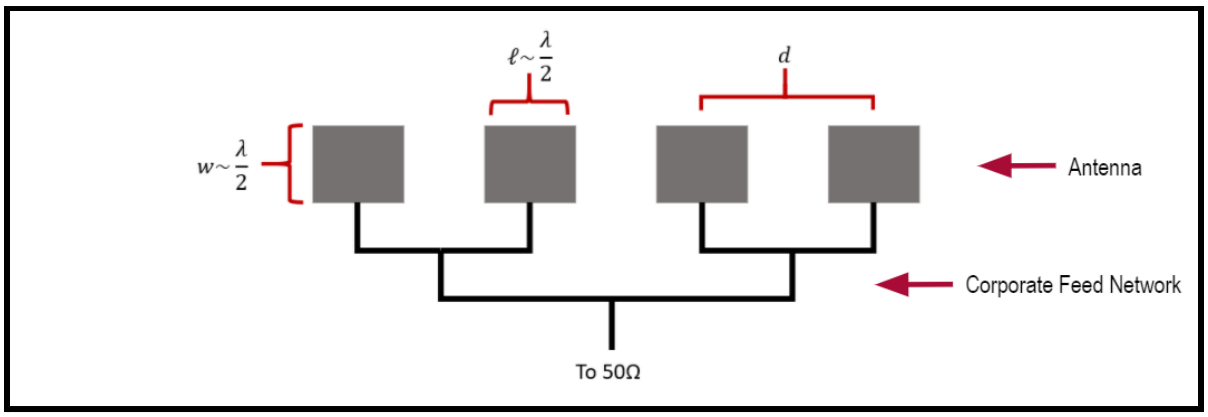

Figure 19: Four element linear antenna array of edge fed half-wavelength microstrip patch antennas

Figure 19 shows our design that utilized a four element linear array. Each grey square represents an individual microstrip patch antenna. The microstrip patch antenna is semi-directional in nature with a ground plane on one side of the antenna that eliminates most of the radiation from the back of the antenna. These individual microstrip patch antennas were then connected together and back to a 50 ohm feed line via a corporate feed network that ensured that the signal passed back and forth remained in phase. Also, the microstrip patch antennas were assembled in a linear array to get an increase in directionality. Generally, more elements in a linear array results in a further increase in directionality. We decided to use four elements. This was a decision based on balancing the size of our antenna with the array directionality increase.

How a linear array affects the radiation pattern of an antenna is defined in Equation 1 below:

$$Eq1:\ E_{total} = E_{element} * AF$$

Where $E_{element}$ represents the radiation pattern of each individual element in the linear array, the array factor (AF) represents the change in radiation pattern from implementing a linear array, and E_{total} is the radiation pattern of the whole antenna system.

The array factor is defined by:

$$Eq2:\ |AF| = \left| \frac{sin\frac{N\Psi}{2}}{sin\frac{\Psi}{2}} \right|$$

where N is the number of elements in the linear array, and Ψ is the phase difference at the observation point of each antenna compared to its neighbor defined in Equation 3:

$$Eq3:\ \Psi = \beta d cos\theta + \alpha$$

where *d* is the interelement spacing, θ is the angle from the array to the emitter, α is the interelement phase shift, and β is the free space wavenumber.

The effect of adjusting the AF through an increase in array elements is shown in Figure 20 below:

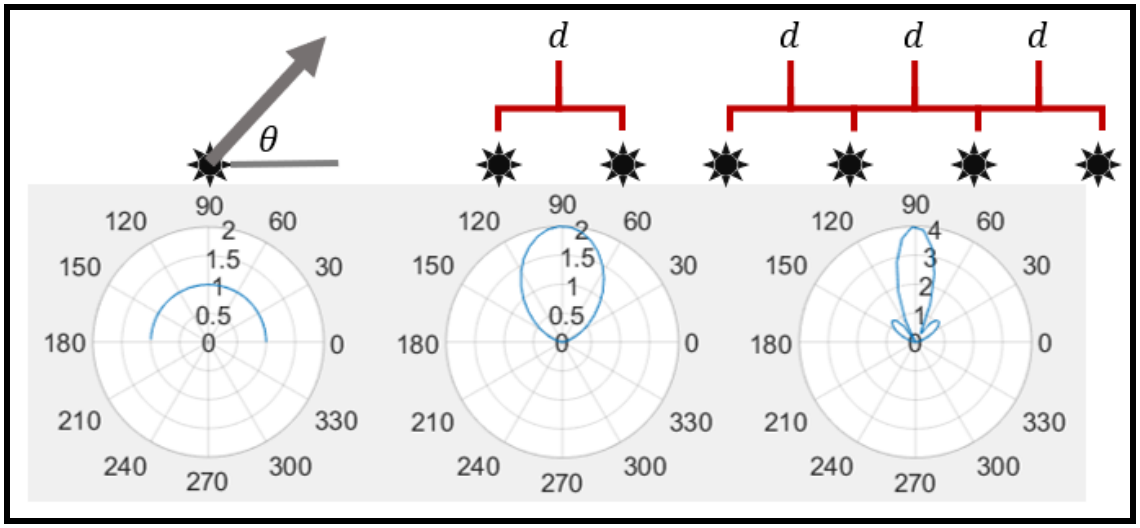

Figure 20: Visual representation of how increasing the number of antenna elements in a linear array would affect the radiation pattern of a linear array of microstrip patch panel antennas

Figure 20 illustrates a top-down view of the radiation pattern of a linear antenna array of microstrip patch antennas. The left picture (N=1) describes a system with only a single element. There is effectively no added AF in this picture. The middle picture (N=2) represents a system with two patch antennas. There is a noticeable increase in directivity from the added second element. The right picture (N=4) shows a system with four elements. Again, there is a clear increase in directionality of the radiation pattern.

The first steps in getting the design dimensions for our antenna were to choose our operating frequency and substrate. Our system was designed to operate within the 5 GHz U-NII band. We decided to choose channel 36 or 5.18 GHz, which is the lowest frequency channel in the band. We chose this channel because it would propagate slightly better in non freespace environments and allow our system to locate an emitter from farther away. The tradeoff was that our components would be slightly larger than if we had chosen a higher frequency channel. The effects of frequency/wavelength will be relevant when design formulas are discussed in subsequent sections.

A substrate is provided by a manufacturer clad between two pieces of copper. The system antenna was created by first printing stickers at the SCU maker lab in the shape of our design and

then using wet etching methods at the SCU chemistry lab to alter the top layer of copper into our antenna design while preserving the continuous ground plane. As this is essentially a microstrip transmission line, it is governed by the associated design equations listed below [7]. The characteristic impedance of a microstrip line is given by the following piecewise function:

$Eq4$:

$$Z_0 = \begin{cases} \frac{60}{\sqrt{\varepsilon_e}} \ln\left(\frac{8d}{W} + \frac{W}{4d}\right) & for\ W/d \leq 1 \\ \frac{120\pi}{\sqrt{\varepsilon_e}\left[\frac{W}{d} + 1.393 + 0.667\ln\left(\frac{W}{d} + 1.444\right)\right]} & for\ W/d \geq 1 \end{cases}$$

Where d is the substrate thickness, W is the microstrip line width, and is the effective impedance given by the following empirical formula:

$Eq5$:

$$\varepsilon_e = \frac{\varepsilon_{r+1}}{2} + \frac{\varepsilon_{r-1}}{2} \frac{1}{\sqrt{1 + 12d/W}}$$

The two main features that determined what substrate we chose were the substrate thickness, *d*, and the relative permittivity, ϵ_r. Relative permittivity is dictated by material properties of the substrate. When determining what substrate type we would use we looked at three different types of Rogers substrates: 5870, 6002, and 6006. The effect of substrate thickness and relative permittivity choices on our microstrip patch length is shown below in Figure 21:

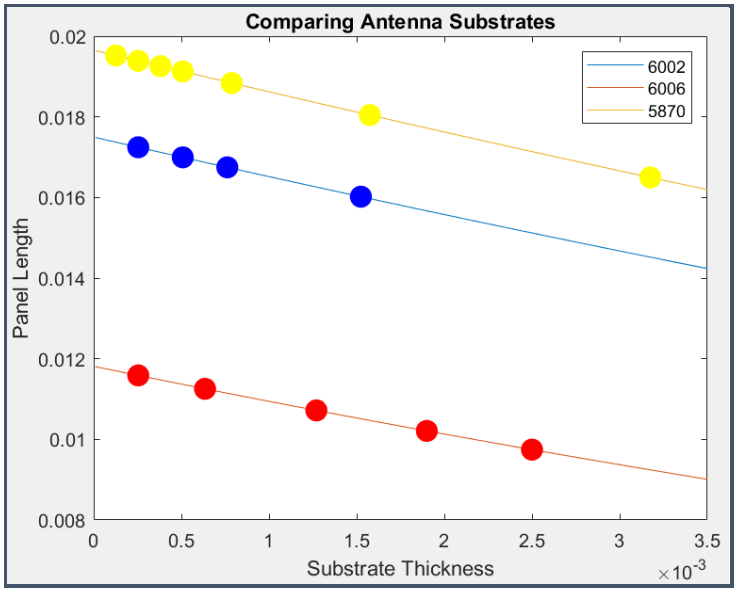

Figure 21: Effect of substrate type and thickness on microstrip patch length

It is important to note that in order for our antenna to function properly the substrate thickness had to be much less than the wavelength. Also, the minimum microstrip line width we were capable of manufacturing via wet etch methods was 200 um. Taking all of this into consideration, we chose to use the Roger 6002 substrate with a thickness of 1.524 mm.

Next, design dimensions for our antenna were researched followed by HFSS simulation and refinement. Design dimensions for a single microstrip patch antenna were used from the *Antenna Theory and Design* textbook [8]. Each microstrip patch element in the antenna has the same dimensions. The resulting design dimensions for the upper part of the antenna are shown below in Figure 22:

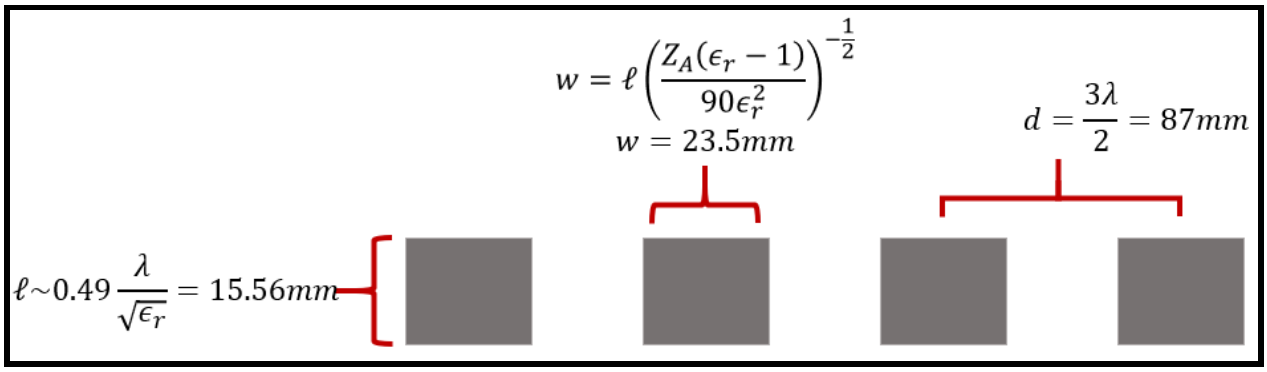

Figure 22: Top portion of antenna design dimensions

We ended up having to increase the spacing between our elements from half a wavelength to three halves of a wavelength in order to avoid coupling between the elements that made it difficult to get a desirable match at our design frequency. The quality of match was determined using the S_{11} (S11) parameter which is a measure of how much power is reflected back out of the antenna's single port. A low S11 value (in dB) is significant because it indicates that most of the power being received by the antenna is being passed out of its port to a coaxial line and eventually to the RF DF system. At half a wavelength element spacing the max achievable S11 at the design frequency was approximately -14 dB. After increasing the interelement spacing to three halves of a wavelength an S11 lower than -20 dB was achievable. This change did not affect the directionality of our antenna.

Next, the corporate feed network was designed. Quarter wave transformers (QWT) were used to keep our minimum line width above 200 um. The design dimensions calculated for our corporate feed network are shown below in Figure 23:

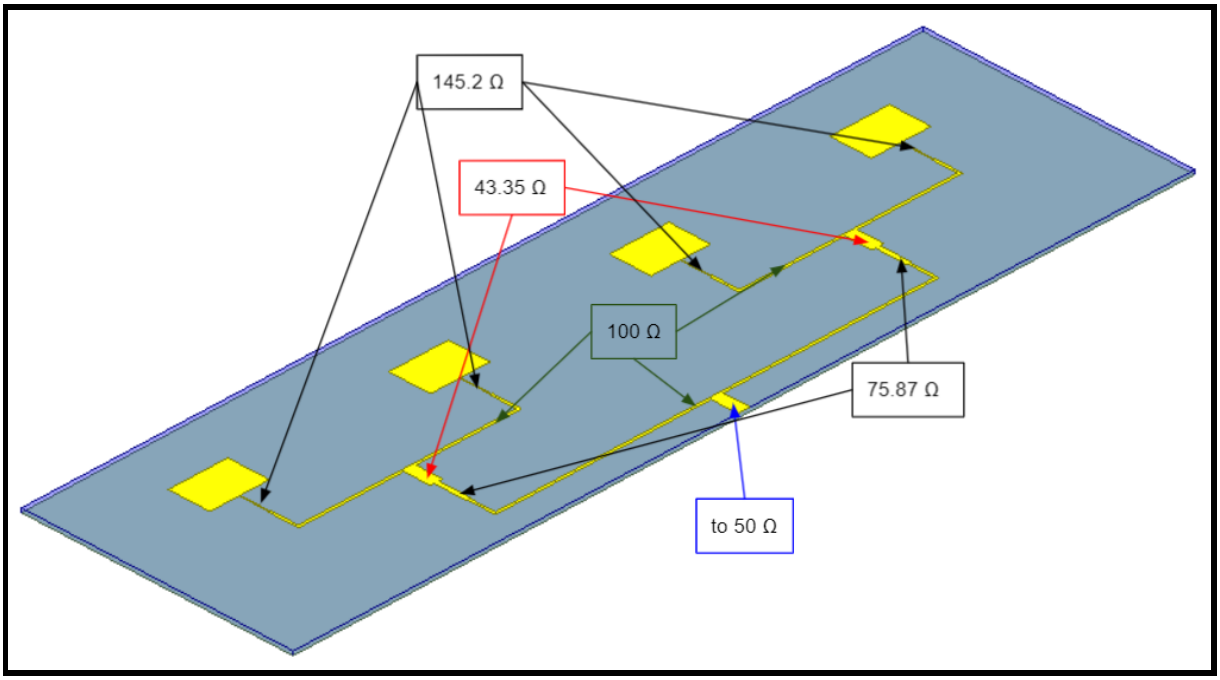

Figure 23: Antenna corporate feed network with QWTs

The QWTs in Figure 23 above are the 145.2 and 75.87 Ohm lines. The limiting feature of this design was the final QWT connected to the microstrip patch. The impedance of 145.2 ohms translated to a line width of 358 um which was above the minimum requirement of 200 microns. Table 1 below shows the vertical design dimensions of the corporate feed network. Microstrip line dimensions are listed from a single microstrip patch to the 50 Ohm feed line.

Microstrip Line	Impedance (Ω)	Width (mm)	Length (mm)
QWT 1	145.2	0.358	11.4
Line 1	100	1.044	10
Line 2	43.35	4.85	10
QWT 2	75.87	1.9	11.4
Line 3	100	1.044	10
Line 4	43.35	4.85	10

Table 1: Corporate feed network vertical microstrip line dimensions starting from microstrip patch and ending at 50 Ohm feed line.

The design values shown in Figures 22, 23, and Table 1 are the refined values after running many HFSS simulations and adjusting to match the antenna to the target frequency. The final match is shown via an S11 plot in Figure 24 below:

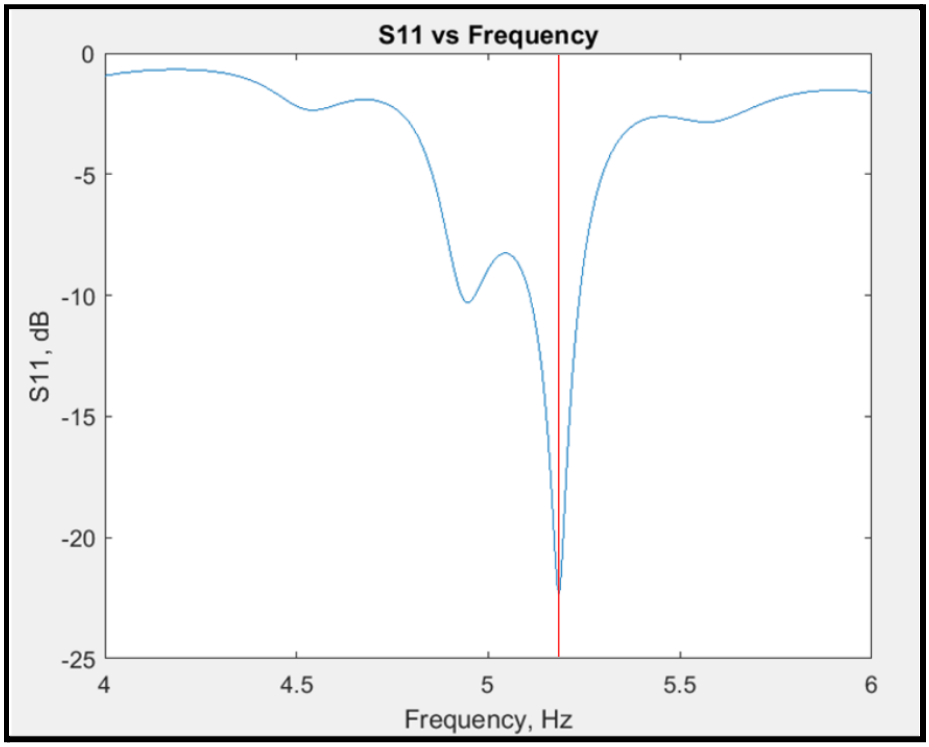

Figure 24: S11 plot showing reflected power based on HFSS simulation, with red line at desired 5.18 GHz

The S11 value at the design frequency of 5.18 GHz is -22 dB. This indicates that over 99% of the received power at that frequency should be passed on to the transmission line connected to the antenna.

The expected radiation pattern of the antenna was verified via HFSS simulation. This is shown in Figure 25 below:

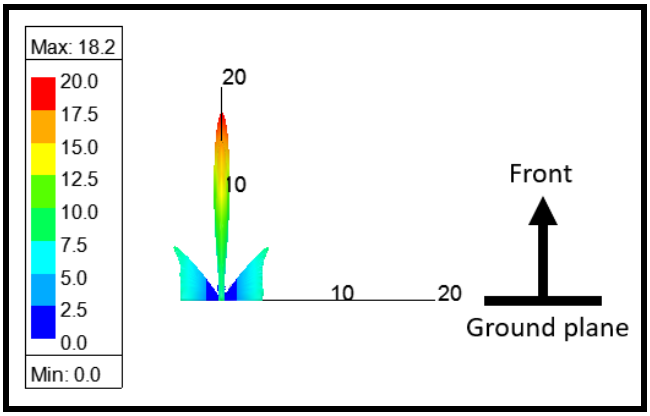

Figure 25: Radiation pattern of antenna from HFSS

Figure 25 shows that the antenna has a very narrow main lobe at its center with some smaller side lobes. This narrow main lobe is essential for our DF capability in terms of determining a difference in signal strength with only a slight movement.

Based on the sample substrate size we received from Rogers Corporation, we were able to manufacture two nearly identical antennas. These two antennas are shown below in Figure 26:

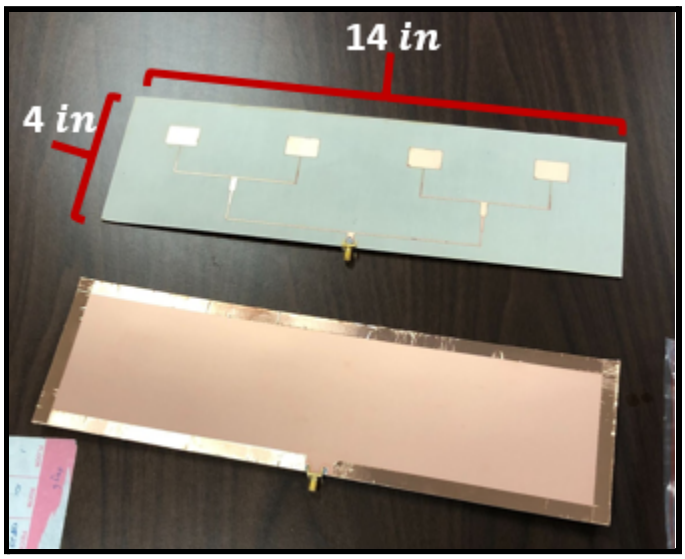

Figure 26: Finished antenna front (top) and back (bottom)

2.7.6.1 Antenna Test:

In order to test our antenna design we measured the reflection coefficient (S11, voltage standing wave ratio (VSWR)) at the target frequency. Ideally, this test would be done in software to find the computational answer and in person with the final antenna array using an oscilloscope. Unfortunately, due to COVID we were unable to gain access to lab equipment to run these physical tests. Instead, we simply set our target emitter to output on the target frequency of 5.18 GHz and took a signal strength measurement with a three dBi gain monopole antenna at approximately six meters distance from our emitter. The recorded signal strength was -40 dBm. We then attached our directional antenna and pointed it at the emitter to achieve maximum gain and took a signal strength measurement of -29 dBm. This would indicate that the max gain of our antenna is approximately 14 dBi at 5.18 GHz which is very close to our HFSS simulated value of 16 dBi. Also, we tested directivity by recording values when the antenna was facing 90 degrees away from the emitter and 180 degrees away from the emitter. At 90 degrees away the RSS dropped by approximately 5 dB and at 180 degrees away it dropped by approximately 10 dB. From this rudimentary testing we can infer that our antenna functions appropriately.

3 Project Outcomes:

3.1 System Integration:

A large portion of this project involved integrating different components. This created many unique unforeseen challenges as we started performing tests and combining more parts. Our system integration processes can generally be broken into two categories: software and hardware. The software portion will include the main Python function and address some software integration issues encountered while the hardware portion will detail physical interfacing of devices.

3.1.1 Software Integration:

3.1.1.1 Main Function:

Our main DF program was coded via Python and overall has a very simplistic functionality. After running the main function, the system will enter an idle state. From there, it will wait for the user to push any key in order to take a measurement. After a key is pressed, the GPS sub function will be called and return a latitude and longitude value. Next, the motor will rotate 360 degrees in the clockwise direction. At three degree increments measurements will be taken and a compass value will be recorded with its associated RSS value. After this is finished, the motor will rotate back to the starting position. Subsequently, all of the recorded RSS values will be compared and the highest value will be returned to the operator with its associated compass direction. Thus, the end result will be both a compass direction and RSS in dBm. The described process is illustrated below in Figure 27:

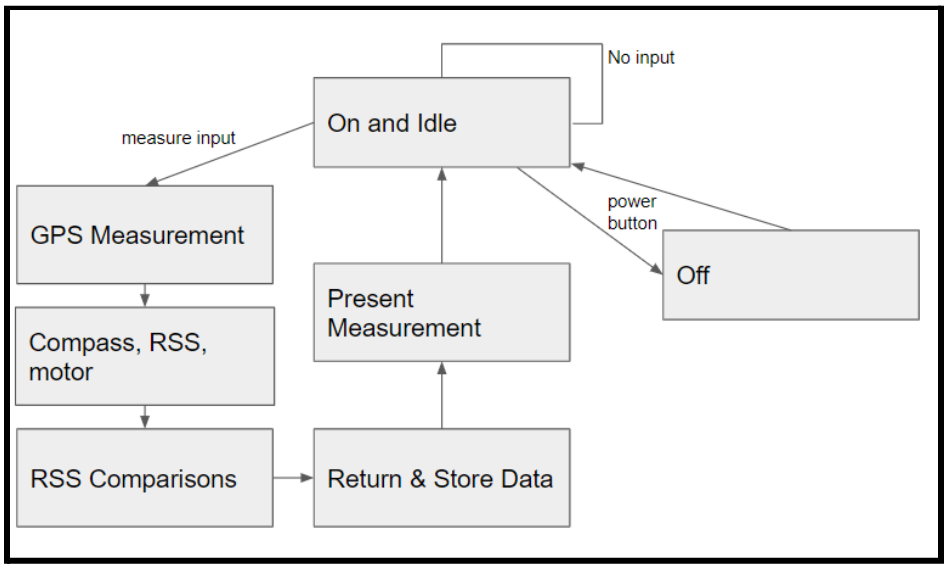

Figure 27: Basic program functionality

3.1.1.2 Known Software Problems:

One of the main issues we encountered was running code on different versions of Python. Certain vendor provided functions required specific versions of Python that other functions were

incompatible with. An example of this was the GPS sub function. It was designed to be used with an older version of Python that was incompatible with the vendor provided code for the stepper motor. This is an open issue that will need to be resolved in the future.

3.1.2 Hardware Integration:

3.1.2.1 Attaching Peripheral Components:

Most of the components used were USB devices and were easy to physically integrate. However, the compass did require using the GPIO pins of our Raspberry Pi which were passed to other pins via the motor controller hat. Both the motor controller and compass did require some soldering to mount correctly. The mounting of the motor controller, compass, and other USB peripherals is shown below in Figure 28:

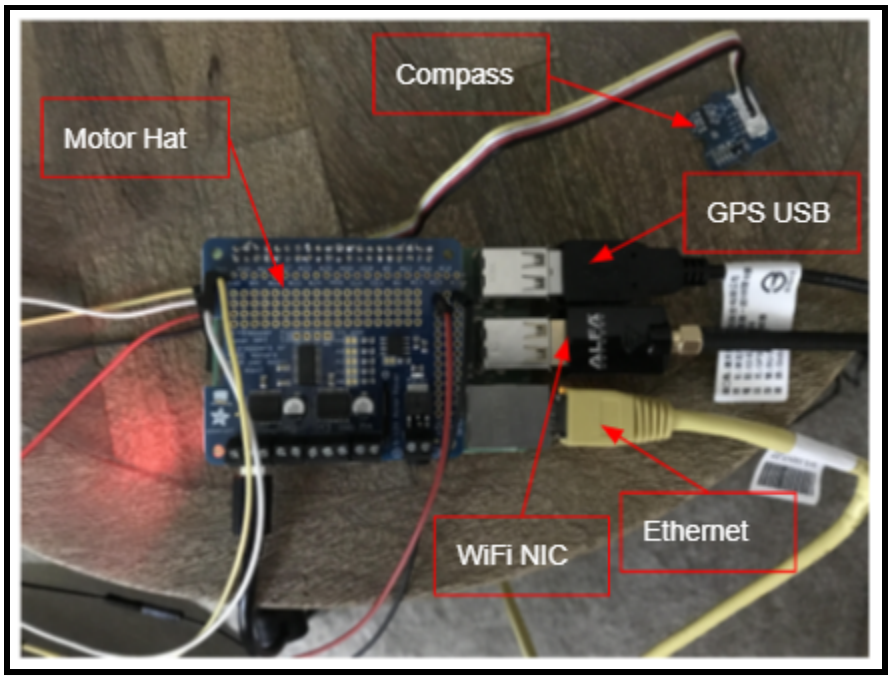

Figure 28: System with attached peripherals

Mounting the antenna to the motor presented another hardware integration consideration. This task was completed by using a U-bracket and mounting the antenna upside down. The mounted antenna is shown below in Figure 29:

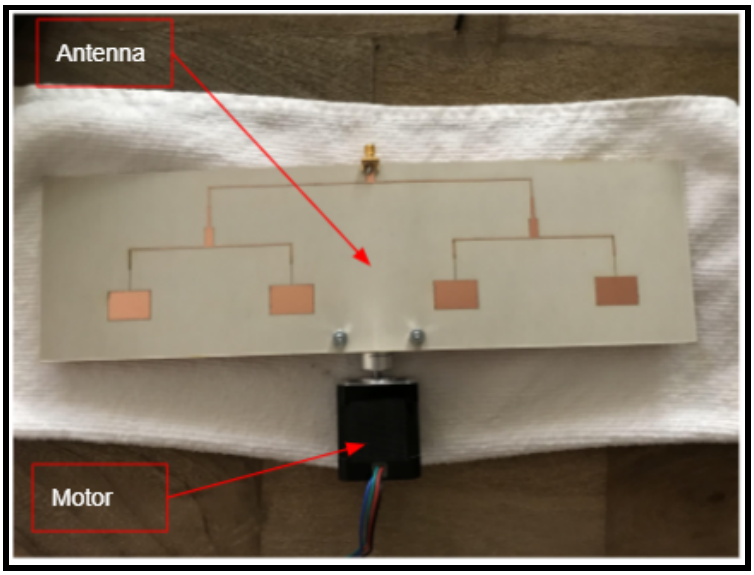

Figure 29: Antenna mounted to motor

By attaching the electronic compass such that the y-axis arrow is facing towards the front of the antenna and also connecting the WiFi NIC to the antenna via a coaxial cable we arrived at our completed system prototype. This is shown below in Figure 30:

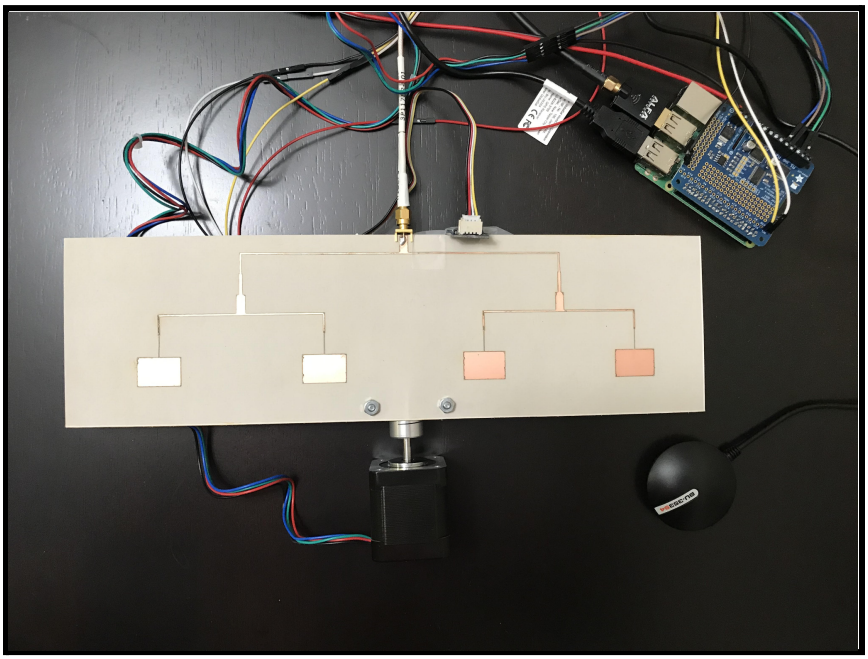

Figure 30: Complete system prototype

3.1.2.2 Known Hardware Problems:

The two main hardware issues we encountered stem from our stepper motor being too weak and also the quality of the stepper motor HAT. The stepper motor performed well in rotation tests with no load attached. However, when the antenna is mounted to it, it cannot handle the load appropriately. This results in the stepper motor being unable to move in controllable steps. This problem is exacerbated when the coaxial cable is attached to the antenna. The coaxial cable resists the motor's movement. This results in the motor stalling and generating heat. An attempted solution to this issue was to incorporate a thinner coaxial cable and run it directly above the antenna. This solution reduced the antenna's resistance to being moved slightly but ultimately did not solve the problem. A separate problem encountered was the stepper motor HAT performing unreliably. Upon initial power on and operation the HAT worked appropriately. However, after about an hour of operation it begins to act erratically by sending commands to the stepper motor when no code is running. A solution to this issue has not been discovered yet. Also, the motor HAT would sometimes cause the electronic compass to reset. This was discovered and verified by running the compass independently of the HAT and then running the compass with the HAT.

3.2 DF Capability:

When testing the capability of our system the main constraints we faced were non-ideal testing conditions and motor issues. Due to COVID-19, we were not able to gain access to labs or other more uniform testing areas. Therefore, our systems capabilities were tested in Jacob’s apartment instead. This presented some difficulties because an apartment complex is an extremely signal dense environment and there were many other objects randomly placed throughout the apartment that caused multipath and absorption. The signal density problem was solved by targeting the beacon name to avoid co-channel interference but the multipath and absorption issues could not easily be addressed given we had no control environment to compare against. The next constraint, the motor being too weak, was a much bigger issue. In order to meet the goal of direction finding within six degrees of accuracy we required the ability to rotate the antenna in small increments (less than six degrees). Unfortunately, our motor was too weak and could not rotate our antenna reliably. Thus, we were unable to perform a DF test via the motor

and had to do it by hand instead. This did not allow us to take small enough measurements to meet our six degree accuracy requirement. However, it did allow us to get within about 10 degrees of accuracy and prove that our system works. The testing layout and a plot showing the direction of the emitter is shown below in Figure 31:

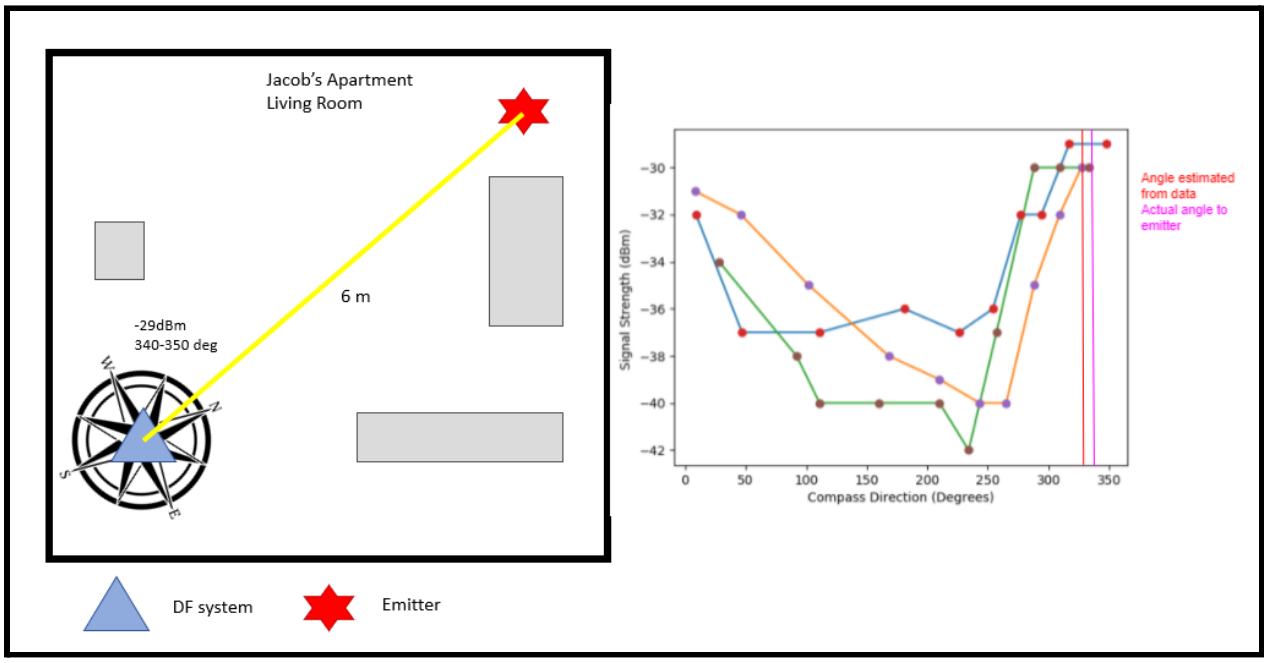

Figure 31: DF testing layout in Jacob's apartment (left). Grey boxes represent objects in the room. Results of three full rotations of the system antenna (right).

3.3 Objective Evaluation:

When evaluating our objectives, we considered three possible outcomes: 'we achieved it,' 'we have what we need to achieve it,' and 'we did not achieve it.'

We theoretically achieved the ability to DF to a range of 200 meters. In order for the system to work properly it needs to be able to receive a signal throughout a full antenna rotation. Thus, the system is limited by the RSS when the back of the antenna is facing the emitter and the receive sensitivity of the USB NIC (-80 dBm). In order to verify that the system could theoretically work on an emitter 200 meters away the ground plane was pointed towards the emitter and an RSS value of -40 dBm was obtained at 6 meters distance. These values were then

extrapolated out to 200 meters using free space path loss equations. Based on these calculations, at a range of 200 meters the RSS of the emitter should be -70dBm. This is greater than the receive sensitivity of the system.

We were not able to achieve the desired level of granularity within a sweep. We had planned to rely on the motor's ability to step at the smallest increment of 1.8°. However, due to issues encountered with the motor and HAT we could not reliably make the motor step through at the desired turn rate. This was why we could not achieve the desired degrees of accuracy.

We achieved the ability to display our data values in real time. While we were not able to incorporate the UI as originally envisioned, we were able to display the data generated via print statements in a terminal and plots. The data display provided both a compass direction and associated RSS value in dBm as originally intended.

Placing the locations of each measurement on the map is an achievable process from the data we currently have. However, due to time constraints, the other more fundamental goals were prioritized. Thus, we did not get the chance to implement this functionality yet.

The lightweight characteristic of our system should be easily implementable with a plastic casing to house our system components with the exception of the antenna. The antenna could be mounted on top of the casing such that it has enough room to freely rotate. The system weighs two pounds, and adding a simple box to house our device would not add more than one pound, which still leaves our device easily held in one hand with the antenna protruding from the top of the system.

The aforementioned goals and their statuses are described below in Table 2:

Goal:	Achievement:	Status:
DF to a range of 200 m away	Achieves 200 meters based on theory	✓
DF within 6 degrees of accuracy	Motor struggles with precise movement in setup	✗
Display DF data in real time with measurements	Data values displayed, UI not configured	✓
Place locations on map upon later return	GPS and Compass allow for this type of review, but actual map not actualized	✓
Lightweight and easily carryable by one person	Size and weight of device easily carryable by one person	✓

Table 2: Basic evaluation of goals

3.4 Future Work:

The main three tasks that still need to be completed for this project are upgrading the motor and controller, implementing a UI, and enclosing the system in an easily carryable case. The budget for the motor needs to be increased significantly in order to purchase a higher caliber motor that is capable of rotating our antenna in a smooth and precise manner. The motor controller we purchased was also unreliable and needs to be upgraded.

We originally had plans to implement a UI but unfortunately ran out of time to complete this portion. The original plan involved using a simple small screen that would attach to the top of the Raspberry Pi. This screen also has three buttons and a joystick. The screen is depicted below in Figure 32:

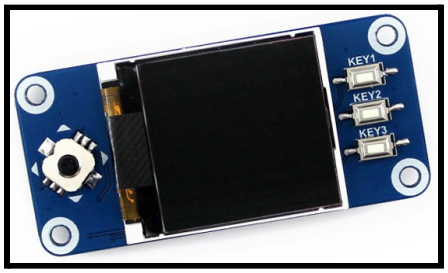

Figure 32: UI screen [18]

The original plan was to set one of the buttons to power on/off and another button that would tell the system to take a measurement. The results of each measurement would be displayed in a bar for signal strength and an arrow indicating the compass direction of the emitter. This is depicted below in Figure 33:

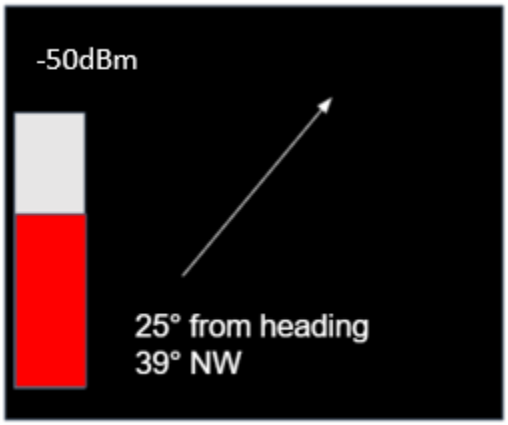

Figure 33: Future UI display plan

Lastly, our entire system needs to be enclosed in a manner that it is easily carryable by an individual. Our individual components are well within our weight limit requirement (3 pounds). However, given that our antenna is wider than anticipated, our system will be larger than originally desired (5''X5''X4''). Thus, we will likely be able to meet our original weight requirement but not our size requirement.

3.5 Risk Analysis and Mitigation Strategies:

In order to determine the risk associated with an activity the likelihood of an event occurring was determined along with its potential consequence. Both the likelihood of an event occurring and its consequences were rated on a scale of one through five. The different risk factors were rated using a collaborative approach. Each group member suggested what they thought the factor should be rated at and then these values were averaged. The matrix shown below (Figure 34) was used to assess the risk associated with each individual risk item of our senior design project.

		Consequence				
		Negligible 1	Minor 2	Moderate 3	Major 4	Catastrophic 5
Likelihood	5 Almost certain	Moderate 5	High 10	Extreme 15	Extreme 20	Extreme 25
	4 Likely	Moderate 4	High 8	High 12	Extreme 16	Extreme 20
	3 Possible	Low 3	Moderate 6	High 9	High 12	Extreme 15
	2 Unlikely	Low 2	Moderate 4	Moderate 6	High 8	High 10
	1 Rare	Low 1	Low 2	Low 3	Moderate 4	Moderate 5

Figure 34: Risk assessment matrix [9]

Overall, five potential risk items were identified:

1. **Batteries:** Our system is designed to be powered via batteries. High voltage batteries can be a hazard. However, our system will run off of AA batteries. AA batteries supply approximately 1.5 V which is not high enough to be considered dangerous. Therefore, this is not a risk item.

2. **COVID-19:** The COVID-19 pandemic represents a potential hazard to our team and project because it greatly hinders our ability to utilize lab spaces and work collaboratively. Due to lockdown restrictions, only a limited number of students are allowed on campus. This presented a low risk to our project success by making it difficult to physically integrate and test our system using lab equipment. However, we deemed the consequence to be negligible because we were able to develop alternative methods to testing that did not require specialized SCU lab equipment.

3. **Servo/Motor:** Our system is designed in such a way that it requires an electric motor/servo to rotate an antenna. This motor is a potential hazard because it may cause bodily harm if someone were to touch it while it is operating. However, because our

system is relatively small and the antenna that will be rotated is also small, this motor does not need to be very powerful. Thus, the likelihood of this actually causing harm is rare and the consequence is negligible. This results in an overall risk of low. This risk was further mitigated by wearing gloves when operating the electric motor when necessary.

4. **Transmitting RF:** Testing our system will require using an emitter of some sort. Transmitting RF can be hazardous at high power levels because it can cause RF burns from touching transmitting antennas and potentially cause cancer from prolonged exposure. However, we used a FCC compliant 5 GHz Wi-Fi router to test our system. The FCC outlines strict transmit power regulations that are safe. Thus, this is not a risk item.

5. **Soldering:** The assembly and integration of our system components required some soldering. Soldering can be hazardous to the eyes and skin. We determined that the likelihood of damaging our skin or eyes is unlikely and that the consequence is minor. This results in an overall risk of moderate. However, because we wore the appropriate protective equipment (goggles and gloves), the likelihood was reduced to rare and the consequence to negligible. This effectively reduced the risk from moderate to low.

Combined Risk Associated with Project: Overall, when taking the five listed risk items into consideration and using the appropriate protective equipment, the risk associated with our senior design project was **low**.

3.6 Ethical Considerations:

There are two primary ethical considerations with our RF DF system: eavesdropping and hacking/tracking. Both of these items revolve around misusing our system. Eavesdropping involves violating people's privacy by listening to their communications. Fortunately, our system is designed in such a way that it is incapable of decoding the information being passed on the channel it is locating. The signal strength is the only thing that is recorded. Therefore, it is not feasible to eavesdrop using our system. The other ethical consideration for our system is that it

may be used in conjunction with hacking or tracking activities. This ethical consideration has been mitigated by designing our system such that it is extremely specific. Our RF DF system only has the ability to locate a single channel within the 5 GHz U-NII band. This limits the ability of people to misuse our system. However, there is no way to prevent our system being used for nefarious tracking purposes.

3.7 Sustainability:

There are a couple different ways to think about the sustainability of our device over its lifetime. If the device were to be produced and sold commercially, it would be competitive and simple to produce. The device cost less than $200. If this price is between 10-20% of the total cost to fabricate our product, that would put us in the $1000-2000 range, which is where many current DF devices are situated, making us price competitive. For example, the Hammerhead Radio Direction Finder [19] is a system currently on the market that provides less capability than our system and is priced at $995. Similarly, our device is compartmentalized making it easy to interact with when parts are not working so that an individual piece is replaceable with no modifications to any of the code or setup of other components in the device. If our device were to experience failure with a single component, the component is easily replaceable without the need for complete system replacement.

3.8 Professional Issues and Constraints:

The most obvious constraint placed on our project was the amount of time we had to work in person due to the COVID-19 pandemic. Our project had a sizable physical aspect of system construction and integration. It was highly questionable whether or not our team would be able to meet in person at all during the year; this shaped how we went about implementing our project. We decided that the best way to advance with our design was in a decentralized environment, so that tasks could more easily be divided between the two of us. This meant that we picked parts that would be sent to each of us with the responsibility of working on each part assigned to the person that physically had the part. Luckily, we were able to reconvene at the start of spring quarter to assemble all of our components into a single product.

3.9 Conclusions:

The feasibility of our originally envisioned design was validated: a lightweight system capable of locating a one watt emitter up to 200 meters away using the RSS method. The system was able to tell what direction it was facing because of the compass and where it was when the measurement was taken due to the GPS. With the antenna being spun by hand, our system worked as it was expected to and returned the direction with the highest RSS.

The system had several core problems that inhibited its ability to work. The first among these was that the motor was not strong enough to be able to reliably rotate the antenna in consistent step sizes. This was in part due to troubles with the motor HAT. The motor HAT would send fake pulses to the motor causing it to make a ticking sound and to heat up without actually moving. Another issue was encountered in that neither member of our team was knowledgeable enough with Python to convert the GPS files from Python 2 to Python 3. A more experienced programmer would have been able to solve this issue, but it was set aside as more pressing concerns were worked on. Also, a problem was encountered with the motor HAT that caused communication issues with the digital compass, often causing the program to crash because the compass would be reset in the middle of a run. For this reason and the one above about the motor, the motor HAT was abandoned from the project.

Throughout this project we learned a lot about the engineering design process and discovered many changes that could have been made to better achieve our goals. The primary change would be to invest in a better control device for the motor. The motor HAT was the weakest point of the project as it caused numerous problems for the motor and the compass, while only being moderately useful as a controller. This part was selected for its affordability, but in the future a higher quality part should be selected. Another improvement to the design process would be a better evaluation of the strain placed on the motor. The motor was strong enough to move the mass we had originally designed it for, but the actual strength of the motor was less than we had anticipated. A better evaluation of the sources of torque on our motor would lead to a more adequate motor choice for this project.

References:

[1] Noger, Anritsu, Villebon-sur-Yvette. “Locating Sources Of Interference.” Microwave Journal. https://www.microwavejournal.com/articles/23280-locating-sources-of-interference

[2]“Radio Frequency Bands”, Accessed on: Dec. 2, 2020. [Online]. Available: https://terasense.com/terahertz-technology/radio-frequency-bands/

[3]Schantz, Hans. (2011). On the origins of RF-based location. 21 - 24. 10.1109/WISNET.2011.5725029.

[4] Praemittas Systems LLC, Chantilly, VA, USA. *Mongoose Cooperative Digital Direction Finding System*. Available: https://www.praemittias-systems.com/wp-content/uploads/2017/06/MONGOOSE_Slicksheet.pdf

[5] TELEGRID Technologies Inc, Florham Park, NJ, USA. Direction Finding using Software-Defined Radio. Available: https://telegrid.com/wp-content/uploads/2018/10/TELEGRID-IEEE-Presentation-DF.pdf

[6] R. Roy and T. Kailath, "ESPRIT-estimation of signal parameters via rotational invariance techniques," in IEEE Transactions on Acoustics, Speech, and Signal Processing, vol. 37, no. 7, pp. 984-995, July 1989, doi: 10.1109/29.32276.

[7] R. Schmidt, "Multiple emitter location and signal parameter estimation," in IEEE Transactions on Antennas and Propagation, vol. 34, no. 3, pp. 276-280, March 1986, doi: 10.1109/TAP.1986.1143830.

[8] D. M. Pozar, *Microwave engineering*. Hoboken, NJ: John Wiley, 2012.

[9] W. L. Stutzman and G. A. Thiele, Antenna theory and design. Hoboken, NJ: Wiley, 2013.

[10] Kaya, Gulsum Kubra. “Risk Matrix.” Researchgate. https://www.researchgate.net/figure/A-standard-risk-matrix_fig7_323570642

[11] EDUP Electronics Technology Co. Ltd, Shenzhen, China. *2017 NEW MODEL 802.11AC DUAL BAND AC600 WIRELESS USB ADAPTER NETWORK CARD Product Model: EP-AC1635.* Available: https://www.szedup.com/product-item/2017-new-model-802-11ac-dual-band-ac600-wireless-usb-adapter-network-card/#tab-id-2-active

[12] Alfa Network Inc., Taipei City, Taiwan. *AWUS036ACS.* Available: https://www.alfa.com.tw/products/awus036acs?variant=36473965969480

[13] STEPPERONLINE Inc., New York, NY, USA. *STEPPERONLINE Nema 17 Stepper Motor Bipolar 2A 59Ncm(84oz.in) 48mm Body 4-lead W/ 1m Cable and Connector compatible with 3D Printer/CNC.* Available: https://www.amazon.com/STEPPERONLINE-Stepper-Bipolar-Connector-compatible/dp/B00PNEQKC0

[14] Adafruit Industries, New York, NY, USA. *Adafruit DC & Stepper Motor HAT for Raspberry Pi - Mini Kit PRODUCT ID: 2348*. Available: https://www.adafruit.com/product/2348

[15] Raspberry Pi Foundation, Cambridge, United Kingdom. *Raspberry Pi 3 Model B+*. Available: https://www.raspberrypi.org/products/raspberry-pi-3-model-b-plus/

[16] Seeed Technology Co., Ltd, Shenzhen, China. *Grove - 3-Axis Digital Compass V2.* Available: https://www.seeedstudio.com/Grove-3-Axis-Digital-Compass-V2.html?gclid=Cj0KCQjw2NyFBhDoARIsAMtHtZ4ozkgLN8Ovj6diVJkRA-ZewHN08J3MWPYyTa8-UcuNJWZGBXqBK6oaAtfqEALw_wcB

[17] USGlobalSat Inc, New Taipei City, Taiwan. *GlobalSat BU-353-S4 USB GPS Receiver (Black).* Available: https://www.amazon.com/GlobalSat-BU-353-S4-USB-Receiver-Black/dp/B008200LHW

[18] Waveshare Electronics, Shenzhen, China. *128x128, 1.44inch LCD display HAT for Raspberry Pi.* Available: https://www.waveshare.com/1.44inch-lcd-hat.htm

[19] Landfall Navigation, Stamford, CT, USA. *Hammerhead Radio Direction Finder.* Available: *https://www.landfallnavigation.com/rdf-hammerhead-v3-radio-direction-finder.html?gclid=Cj0KCQjw--GFBhDeARIsACH_kda9MYnXsvzxtNxfb-hcoMbEqM-rS_D3PMjH3GdNp20oS_zC6oVbpiwaAkDHEALw_wcB*

Appendices

Appendix 1: Equipment and Software used

Design Tools and Software:

Tool:	*Purpose:*
High-Frequency Structure Simulator (HFSS)	Full-wave circuit simulator used for creation of Antenna
Python	Coding language for system on Raspberry Pi

Table 2: Tools and software used to help design RF DF system

Equipment:

Equipment:	*Purpose:*
Laptop or desktop computer	Used in conjunction with NIC to test antenna
5 GHz capable Wi-Fi router	Generates signal to test system against

Table 3: Equipment used to design RF DF system

Appendix 2: Components, Materials, and Budget

Item:	*Explanation:*	*Cost ($):*
Raspberry Pi 4	Microprocessor	44.99
Raspberry Pi power supply	Power the Pi	9.95
Display screen hat	Displays data from measurements	11.99
Micro SD	Primary memory for Pi	7.49
SD card reader	Interface with computer to image SD card	7.99
Stepper Motor	Rotates antenna	15.99
Stepper Motor Hat	Controles Motor	22.50
Hat power supply and adapter	Provide power to stepper motor hat	17.08
USB GPS	Geotags data	30.23
Electronic Compass	Provide current bearing	7.90
USB WiFi NiC	Transfer signal from antenna to Pi	13.99
Antenna	Receives emitter signal, fabricated in house	0*
Total Cost		**190.10**

Table 4: Part costs and total expenditure for RF DF system

*Free sample from Rogers for board and in house fabrication to avoid fabrication costs